

## LETTERS

# Discovery of $^{40}\text{Mg}$ and $^{42}\text{Al}$ suggests neutron drip-line slant towards heavier isotopes

T. Baumann<sup>1</sup>, A. M. Amthor<sup>1,2</sup>, D. Bazin<sup>1</sup>, B. A. Brown<sup>1,2</sup>, C. M. Folden III<sup>1</sup>, A. Gade<sup>1,2</sup>, T. N. Ginter<sup>1</sup>, M. Hausmann<sup>1</sup>, M. Matoš<sup>1</sup>, D. J. Morrissey<sup>1,3</sup>, M. Portillo<sup>1</sup>, A. Schiller<sup>1</sup>, B. M. Sherrill<sup>1,2</sup>, A. Stolz<sup>1</sup>, O. B. Tarasov<sup>1,4</sup> & M. Thoennessen<sup>1,2</sup>

A fundamental question in nuclear physics is what combinations of neutrons and protons can make up a nucleus. Many hundreds of exotic neutron-rich isotopes have never been observed; the limit of how many neutrons a given number of protons can bind is unknown for all but the lightest elements<sup>1</sup>, owing to the delicate interplay between single particle and collective quantum effects in the nucleus. This limit, known as the neutron drip line, provides a benchmark for models of the atomic nucleus. Here we report a significant advance in the determination of this limit: the discovery of two new neutron-rich isotopes— $^{40}\text{Mg}$  and  $^{42}\text{Al}$ —that are predicted to be drip-line nuclei<sup>2</sup>. In the past, several attempts to observe  $^{40}\text{Mg}$  were unsuccessful<sup>3,4</sup>; moreover, the observation of  $^{42}\text{Al}$  provides an experimental indication that the neutron drip line may be located further towards heavier isotopes in this mass region than is currently believed. In stable nuclei, attractive pairing forces enhance the stability of isotopes with even numbers of protons and neutrons. In contrast, the present work shows that nuclei at the drip line gain stability from an unpaired proton, which narrows the shell gaps and provides the opportunity to bind many more neutrons<sup>5,6</sup>.

The experimental determination of the neutron drip line is extremely challenging primarily because isotopes at the drip line, for example, perhaps 18 neutrons beyond the stable aluminium isotope, can be produced only in minute quantities if they are accessible at all. The other difficulty is that these nuclei are very fragile, and they

rapidly and preferentially emit neutrons when produced in any nuclear reaction. The theoretical prediction of the drip line is also very difficult because of the lack of a reliable universal theory of the atomic nucleus. From the many theoretical models that are available we selected two of the best global models, the finite range droplet model (FRDM) and the Hartree–Fock–Bogoliubov model. Figure 1 shows the predicted neutron drip line from these two models and illustrates the large variation in model predictions. The FRDM uses a semi-classical description of the macroscopic contributions to the nuclear binding energy augmented with microscopic corrections resulting from local single-particle shell structure and the pairing of nucleons<sup>7</sup> (Fig. 1, solid black line). For comparison, the fully microscopic Hartree–Fock–Bogoliubov model (HFB-8) is a state-of-the-art quantum mechanical calculation<sup>8</sup> that puts the nucleons into a mean field with a Skyrme interaction in which the pairing field is included in analogy to the Bogoliubov–de Gennes equations in condensed matter physics<sup>9</sup> (Fig. 1, dashed green line). We selected HFB-8 over other HFB models because it has the best overall fit to measured masses<sup>10</sup>. Although both FRDM and HFB-8 correctly predict the location of the neutron drip line in many cases, they are not able to account for the detailed interplay of valence protons and neutrons. The discrepancies between the models are particularly large in the region from magnesium to silicon. This issue is especially relevant to the current effort to determine the limits of nuclear existence and the ability to determine those limits with the next generation of nuclear

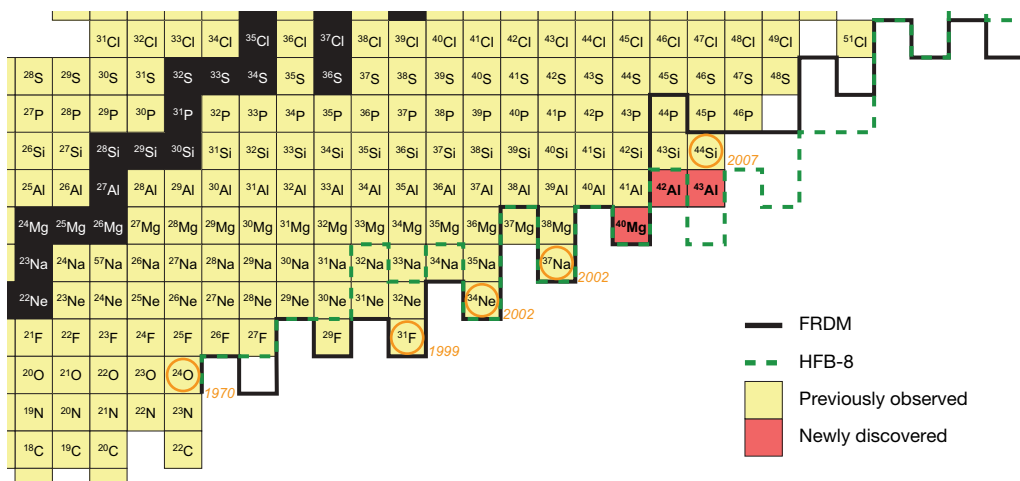


**Figure 1 | Section of the chart of nuclides for light, neutron-rich nuclei.** The proton number increases vertically and the neutron number horizontally. Yellow squares denote previously observed nuclei. The neutron drip lines predicted by the FRDM and HFB-8 models are shown by the black and

dashed green lines, respectively. The most recently observed drip-line nuclei are indicated by orange circles with their year of discovery, and the isotopes discovered in the present experiment are highlighted in red (see the text for details).

<sup>1</sup>National Superconducting Cyclotron Laboratory, <sup>2</sup>Department of Physics and Astronomy, <sup>3</sup>Department of Chemistry, Michigan State University, East Lansing, Michigan 48824, USA. <sup>4</sup>Flerov Laboratory of Nuclear Reactions, JINR, 141980 Dubna, Moscow region, Russian Federation.

research facilities such as the Facility for Antiproton and Ion Research (FAIR) in Europe, the Radioisotope Beam Factory (RIBF) in Japan and the Facility for Rare-Isotope Beams (FRIB) in the United States.

The current knowledge of the drip line is limited to only the lightest nuclei. The last bound oxygen isotope,  $^{24}\text{O}$  (atomic number  $Z=8$ ), was observed in 1970 (ref. 11). However, the neutron drip line was established for oxygen only in 1997 after the nuclei  $^{25}\text{O}$  to  $^{28}\text{O}$  had been shown to be unbound with respect to prompt neutron emission<sup>12–14</sup>. Subsequently, the isotopes  $^{31}\text{F}$ ,  $^{34}\text{Ne}$  and  $^{37}\text{Na}$  were observed<sup>3,4</sup>, and although it is generally believed that they lie along the drip line, the fact that  $^{33}\text{F}$ ,  $^{36}\text{Ne}$  and  $^{39}\text{Na}$  are indeed unbound has not been experimentally established. These experiments also failed to observe the even–even nucleus  $^{40}\text{Mg}$  and it was speculated that  $^{40}\text{Mg}$  might be unbound<sup>15</sup>. Here we report the production and identification of  $^{40}\text{Mg}$  for the first time, as well as that of the neighbouring odd- $Z$  nucleus  $^{42}\text{Al}$ .

The fragmentation of stable nuclei followed by the separation and identification of the products in less than  $1\ \mu\text{s}$  is the only method currently available to produce nuclei at or near the neutron drip line<sup>1</sup>. The observation of the isotopes of interest requires a high primary-beam intensity, a high collection efficiency, a high efficiency of identification and—perhaps most importantly—a very high degree of purification because they are produced very rarely, in only about 1 in  $10^{15}$  reactions. These requirements are met at the National Superconducting Cyclotron Laboratory<sup>16</sup> at Michigan State University with the use of the A1900 fragment separator<sup>17</sup> and S800 analysis beamline<sup>18</sup>. A primary beam of  $^{48}\text{Ca}$  with an energy per nucleon of 141 MeV was interacted with a  $^{nat}\text{W}$  target, 970  $\mu\text{m}$  thick, placed at the object position of the A1900 fragment separator (see Fig. 2). The near beam-velocity products along with the unreacted primary beam particles were separated first by their momentum-to-charge ratio in the A1900, which accepted a  $\pm 2.5\%$  momentum deviation and had an angular acceptance of 120 mrad by 80 mrad, resulting in a total acceptance of about 23% of the yield. The momentum-selected fragments then passed through an aluminium degrader, 156  $\mu\text{m}$  thick, at the momentum-dispersive midplane that preserved the achromaticity of the separator while providing a physical separation of the remaining reaction products by nuclear charge. The momentum and the isotopic identity of the selected particles (about 1 in  $5 \times 10^{10}$ ) were determined in the S800 analysis system on an event-by-event basis by position measurement of the momentum-dispersed ions. A detector stack consisting of a position-sensitive parallel-plate avalanche counter, seven silicon PIN diodes, 1 mm thick, and a plastic scintillator, 50 mm thick, provided the particle identification, which required consistent energy-loss measurements in all seven silicon detectors and consistent determination of two

flight times over 21 m and 46 m flight paths. After initial calibrations the entire system was set to the expected magnetic rigidity for  $^{40}\text{Mg}$ , corresponding to 4.78 T m after the production target. Data were collected for a total of 7.6 days over an 11-day period; the average incident beam intensity was  $5.0 \times 10^{11}$  particles per second.

The particle identification can be seen in Fig. 3, where the locus of isotopes with constant  $N=2Z$  is indicated by the vertical line and heavier isotopes lie to the right. Three events of  $^{40}\text{Mg}$  were clearly identified. Each of the parameters that are used for the particle identification has been checked on an event-by-event basis to exclude possible ambiguous background events. The non-observation of any events that would correspond to  $^{39}\text{Mg}$  indicates that it is unbound. The probability that the three events identified as  $^{40}\text{Mg}$  correspond to  $^{38}\text{Mg}$ , on the basis of the distribution of  $^{38}\text{Mg}$  events, is less than  $3 \times 10^{-15}$ . In addition, many events of the previously observed  $^{31}\text{F}$ ,  $^{34}\text{Ne}$  and  $^{37}\text{Na}$  isotopes were detected. The fact that  $^{30}\text{F}$ ,  $^{33}\text{Ne}$  and  $^{36}\text{Na}$  are unbound (lack of events) was also confirmed. Further, the 23 events of  $^{42}\text{Al}$  establish its discovery. Figure 3 also contains one event consistent with  $^{43}\text{Al}$ . We determined a probability of  $2.4 \times 10^{-3}$  that this event was caused by a possible contribution from the neighbouring  $^{42}\text{Al}$ . Furthermore, as a result of the attractive neutron-pairing interaction, the firm observation of the odd–odd isotope  $^{42}\text{Al}_{29}$  supports the existence of  $^{43}\text{Al}_{30}$ , lending credibility to the interpretation of the single event as evidence for the existence of this nucleus. Our experiment also confirmed the recent observation of  $^{44}\text{Si}$  with the A1900 separator<sup>19</sup>.

The discovery of the even–even  $^{40}\text{Mg}$  isotope is consistent with the predictions of both the FRDM and the HFB-8 model and with the staggered pattern of the drip line in this region. It is interesting to note that if the even–even  $^{40}\text{Mg}_{28}$  had not been observed in the present experiment, the drip line might have been considered determined up to magnesium. However, with the observation of  $^{40}\text{Mg}$  the question remains open as to whether  $^{31}\text{F}$ ,  $^{34}\text{Ne}$ ,  $^{37}\text{Na}$  and  $^{40}\text{Mg}$  are the last bound isotopes of fluorine, neon, sodium and magnesium, respectively.

More important than the observation of the even–even  $^{40}\text{Mg}$  is the discovery of the odd–odd  $^{42}\text{Al}$ , which was predicted to be unbound by the FRDM and HFB-8 models. The present observation breaks the pattern of the staggering at the drip line. The addition of one unpaired proton in the  $0d_{5/2}$  orbital to magnesium seems to have a significant influence on the stability of the most neutron-rich isotopes, similar to the transition from oxygen to fluorine. Quantum-mechanical calculations such as HFB-8 and the *sd*fp-shell model<sup>20</sup> predict that the  $1p_{3/2}$  orbital will start to fill at  $N=29$  and that the single-particle energy of the  $1p_{3/2}$  orbital remains more or less constant as a function of neutron number. Our observation of  $^{42}\text{Al}$  therefore suggests that all of the aluminium isotopes up to the

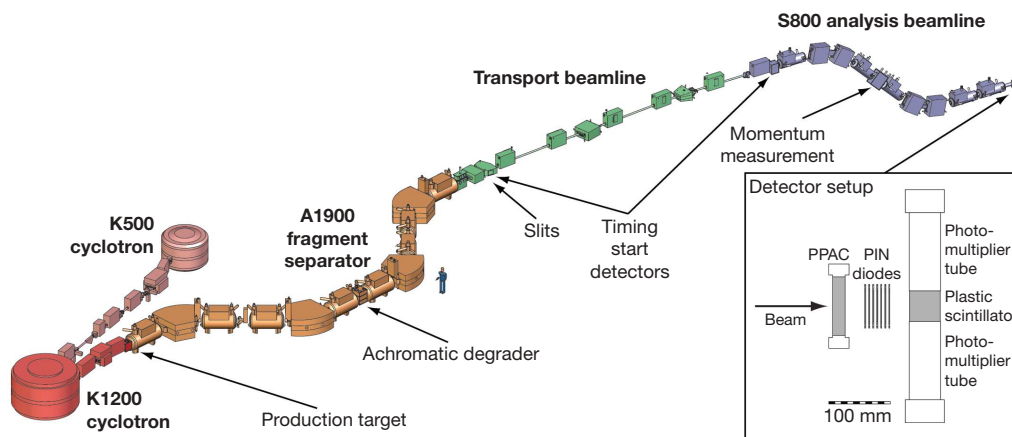


**Figure 2** | Schematic diagram of the coupled cyclotron facility<sup>16</sup>. This overview diagram shows the major components used for the production,

separation and identification of new neutron-rich nuclei. PPAC, parallel-plate avalanche counter.

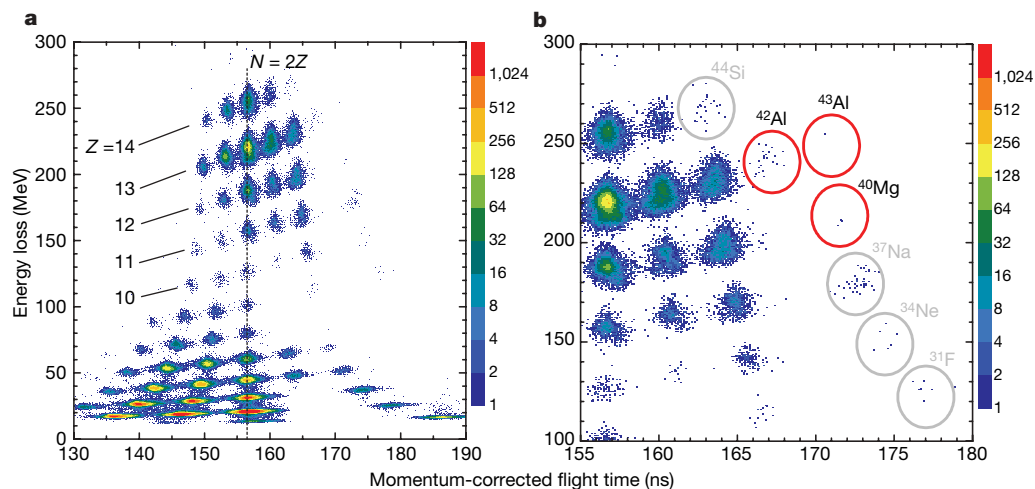


**Figure 3 | Particle identification plots of observed isotopes.** **a**, Particle identification of the neutron-rich products between beryllium and silicon, including the new isotopes  $^{40}\text{Mg}$ ,  $^{42}\text{Al}$  and the single event identified as  $^{43}\text{Al}$ . **b**, Expanded region of heaviest exotic nuclei. The energy loss in the first PIN detector is plotted against the flight time of the nuclei through the S800

analysis line, corrected to the momentum of the central path, indicating the unambiguous identification of each isotope. Isotopes of an element lie on diagonal lines and isotopes with  $N = 2Z$  lie along a single vertical line (dashed line in **a**).

nominal filling of the  $1p_{3/2}$  orbital ( $^{45}\text{Al}_{32}$ ) are most probably bound. Heavier nuclei up to  $^{47}\text{Al}$  are also probably bound if the  $1p_{3/2}-1p_{1/2}$  spin-orbital splitting becomes small, as suggested by the new generation of Skyrme forces that include the tensor interaction<sup>5,6</sup>. This is illustrated by a more recent version of the HFB calculation (HFB-9), which does predict  $^{42}\text{Al}$  to be bound and actually shows even  $^{48}\text{Al}$  to be bound<sup>10</sup>. This demonstrates the likelihood that the drip line is significantly further from stability than predicted by models such as HFB-8, which predict that  $^{42}\text{Al}$  is unbound.

Thus, the observation of  $^{40}\text{Mg}$ ,  $^{42}\text{Al}$  and possibly even  $^{43}\text{Al}$  at or near the neutron drip line provides the first experimental indication that the stability of very neutron-rich aluminium isotopes is enhanced relative to magnesium. This provides a significant advance in our understanding of where the drip line is likely to lie in this region and indicates that it may be farther from stable isotopes than expected. Hence, the goal of defining the limits of stability at the current and next generations of nuclear science facilities built to study rare isotopes may be significantly more difficult than previously believed. In fact, the results of this experiment indicate that the drip line may be beyond the reach of all of these facilities for nuclei with atomic numbers greater than 12.

Received 6 June; accepted 31 August 2007.

1. Thoennessen, M. Reaching the limits of nuclear stability. *Rep. Prog. Phys.* **67**, 1187–1232 (2004).
2. Audi, G., Wapstra, A. H. & Thibault, C. The AME2003 atomic mass evaluation. *Nucl. Phys. A* **729**, 337–676 (2003).
3. Notani, M. *et al.* New neutron-rich isotopes,  $^{34}\text{Ne}$ ,  $^{37}\text{Na}$  and  $^{43}\text{Si}$ , produced by fragmentation of a 64 A MeV  $^{48}\text{Ca}$  beam. *Phys. Lett. B* **542**, 49–54 (2002).
4. Lukyanov, S. M. *et al.* Experimental evidence for the particle stability of  $^{34}\text{Ne}$  and  $^{37}\text{Na}$ . *J. Phys. G Nucl. Part. Phys.* **28**, L41–L45 (2002).
5. Otsuka, T., Matsuo, T. & Abe, D. Mean field with tensor force and shell structure of exotic nuclei. *Phys. Rev. Lett.* **97**, 162501 (2006).
6. Brown, B. A., Duguet, T., Otsuka, T., Abe, D. & Suzuki, T. Tensor interaction contributions to single-particle energies. *Phys. Rev. C* **74**, 061303(R) (2006).

7. Möller, P., Nix, J. R., Myers, W. D. & Swiatecki, W. J. Nuclear Ground-State Masses and Deformations. *At. Data Nucl. Data Tables* **59**, 185–381 (1995).
8. Samyn, M., Goriely, S., Bender, M. & Pearson, J. M. Further explorations of Skyrme-Hartree-Fock-Bogoliubov mass formulas. III. Role of particle-number projection. *Phys. Rev. C* **70**, 044309 (2004).
9. de Gennes, P. G. *Superconductivity of Metals and Alloys* (Addison-Wesley, Reading, Massachusetts, 1989).
10. Goriely, S., Samyn, M., Pearson, J. M. & Onsi, M. Further explorations of Skyrme-Hartree-Fock-Bogoliubov mass formulas. IV: Neutron-matter constraint. *Nucl. Phys. A* **750**, 425–443 (2005).
11. Artukh, A. G. *et al.* New isotopes  $^{21}\text{N}$ ,  $^{23}\text{O}$ ,  $^{24}\text{O}$  and  $^{25}\text{F}$ , produced in nuclear reactions with heavy ions. *Phys. Lett.* **32B**, 43–44 (1970).
12. Langevin, M. *et al.* Production of neutron-rich nuclei at the limits of particles stability by fragmentation of 44 MeV/u  $^{40}\text{Ar}$  projectiles. *Phys. Lett.* **150B**, 71–74 (1985).
13. Guillemaud-Mueller, D. *et al.* Particle stability of the isotopes  $^{26}\text{O}$  and  $^{32}\text{Ne}$  in the reaction 44 MeV/nucleon  $^{48}\text{Ca} + \text{Ta}$ . *Phys. Rev. C* **41**, 937–941 (1990).
14. Tarasov, O. *et al.* Search for  $^{28}\text{O}$  and study of neutron-rich nuclei near the  $N = 20$  shell closure. *Phys. Lett. B* **409**, 64–70 (1997).
15. Lutostansky, Yu. S., Lukyanov, S. M., Penionzhkevich, Yu. E. & Zverev, M. V. Neutron drip line in the region of O–Mg isotopes. *Particles Nuclei Lett.* **115**, 86–93 (2002).
16. Gelbke, C. K. Rare isotope research capabilities at the NSCL today and at RIA in the future. *Prog. Particle Nucl. Phys.* **53**, 363–372 (2004).
17. Morrissey, D. J., Sherrill, B. M., Steiner, M., Stolz, A. & Wiedenhoever, I. Commissioning the A1900 projectile fragment separator. *Nucl. Instrum. Meth. B* **204**, 90–96 (2003).
18. Bazin, D., Caggiano, J. A., Sherrill, B. M., Yurkon, J. & Zeller, A. The S800 spectrograph. *Nucl. Instrum. Methods Phys. Res. B* **204**, 629–633 (2003).
19. Tarasov, O. B. *et al.* New isotope  $^{44}\text{Si}$  and systematics of the production cross sections of the most neutron-rich nuclei. *Phys. Rev. C* **75**, 064613 (2007).
20. Retamosa, J., Caurier, E., Nowacki, F. & Poves, A. Shell model study of the neutron-rich nuclei around  $N = 28$ . *Phys. Rev. C* **55**, 1266–1274 (1997).

**Acknowledgements** This work was supported by the US National Science Foundation.

**Author Information** Reprints and permissions information is available at [www.nature.com/reprints](http://www.nature.com/reprints). Correspondence and requests for materials should be addressed to T.B. ([baumann@nscl.msu.edu](mailto:baumann@nscl.msu.edu)).